Room temperature low-threshold InAs/InP quantum dot single mode photonic crystal microlasers at 1.5 μm using cavity-confined slow light

Frédéric Bordas,[1] **Christian Seassal,**[1] **Emmanuel Dupuy,**[1] **Philipe Regreny,**[1] **Michel Gendry,**[1] **Pierre Viktorovich,**[1] **M. J. Steel,**[2] **and Adel Rahmani**[3]

[1]*Institut des Nanotechnologies de Lyon INL-UMR5270, CNRS, Ecole Centrale de Lyon, Ecully, F-69134, France*

[2] *MQ Photonics Research Centre and CUDOS, Dept of Physics, Macquarie University, NSW 2109, Australia*

[3] *Department of Mathematical Sciences and CUDOS, University of Technology Sydney, NSW 2007, Australia*

f.bordas@tue.nl

Abstract: We have designed, fabricated, and characterized an InP photonic crystal slab structure that supports a cavity-confined slow-light mode, *i.e.* a bandgap-confined valence band-edge mode. Three dimensional finite difference in time domain calculations predict that this type of structure can support electromagnetic modes with large quality factors and small mode volumes. Moreover these modes are robust with respect to fabrication imperfections. In this paper, we demonstrate room-temperature laser operation at 1.5 μm of a cavity-confined slow-light mode under pulsed excitation. The gain medium is a single layer of InAs/InP quantum dots. An effective peak pump power threshold of 80 μW is reported.

OCIS codes: (230.3990) Microstructure devices; (230.5750) Resonators; (140.5960) Semiconductor lasers

References and links

1. J. D. Joannopoulos, R. D. Meade, and J. N. Winn, *Photonic Crystals: Molding the Flow of Light* (Princeton, 1995).
2. K. Sakoda, *Optical Properties of Photonic Crystals* 2nd edition (Springer, 2004).
3. Y. Akahane, T. Asano, B. -S. Song, and S. Noda, "High-Q photonic nanocavity in a two-dimensional photonic crystal," Nature **425**, 944-947 (2003).
4. Y. Akahane, T. Asano, B. -S. Song, and S. Noda, "Fine-tuned high-Q photonic-crystal nanocavity," Opt. Express **13**, 1202-1214 (2005), http://www.opticsinfobase.org/oe/abstract.cfm?URI=oe-13-4-1202.
5. H.-G. Park, J.-K. Hwang, J. Huh, H.-Y. Ryu, S.-H. Kim, J.-S. Kim, and Y.-H. Lee, "Characteristics of Modified Single Defect Two Dimensional Photonic Crystal Lasers," IEEE J. Quantum Electron. , **38**, 1353-1365 (2002).
6. C. Monat, C. Seassal, X. Letartre, P. Regreny, P. Rojo-Romeo, P. Viktorovitch, M. Le Vassor d'Yerville, D. Cassagne, J. P. Albert, E. Jalaguier, S. Pocas, and B. Aspar, "InP based two dimensional photonic crystal on silicon : In plane Bloch mode laser," Appl. Phys. Lett. **81**, p 5102-5104 (2002).
7. A. E. Vasdekis, G. A. Turnbull, I. D. W. Samuel, P. Andrew, and W. L. Barnes, "Low threshold edge emitting polymer distributed feedback laser based on a square lattice," Appl. Phys. Lett. **86**, 161102 (2005).
8. M. Imada, A. Chutinan, S. Noda, and M. Mochizuki, "Multidirectionally distributed feedback photonic crystal lasers," Phys. Rev. B **65**, 195306 (2002).

#105574 - $15.00 USD Received 8 Jan 2009; revised 20 Feb 2009; accepted 22 Feb 2009; published 20 Mar 2009

9. B. Ben Bakir, Ch. Seassal, X. Letartre, P. Viktorovitch, M. Zussy, L. Di Cioccio, and J. M. Fedeli, "Surface emitting microlaser combining two dimensional photonic crystal membrane and vertical Bragg mirror," Appl. Phys. Lett. **88**, 081113 (2006).
10. K. Srinivasan, P. E. Barclay, and O. Painter, "Fabrication-tolerant high quality factor photonic crystal microcavities," Opt. Express **12**, 1458-1463 (2004), http://www.opticsinfobase.org/oe/abstract.cfm?URI=oe-12-7-1458.
11. S.-H. Kwon, S.-H. Kim, S.-K. Kim, and Y.-H. Lee, "Small, low-loss heterogeneous photonic bandedge laser," Opt. Express **12**, 5356-5361 (2004), http://www.opticsinfobase.org/oe/abstract.cfm?URI=oe-12-22-5356.
12. S. Gardin, F. Bordas, X. Letartre, C. Seassal, A. Rahmani, R. Bozio, and P. Viktorovitch, "Microlasers based on effective index confined slow light modes in photonic crystal waveguides," Opt. Express **16**, 6331-6339 (2008), http://www.opticsinfobase.org/abstract.cfm?uri=oe-16-9-6331.
13. F. Bordas, M. J. Steel, C. Seassal, and A. Rahmani, "Confinement of band-edge modes in a photonic crystal slab," Opt. Express **15**, 10890-10902 (2007), http://www.opticsinfobase.org/oe/abstract.cfm?URI=oe-15-17-10890.
14. D. Englund, D. Fattal, E. Waks, G. Solomon, B. Zhang, T. Nakaoka, Y. Arakawa, Y. Yamamoto, and J. Vučković, "Controlling the Spontaneous Emission Rate of Single Quantum Dots in a Two Dimensional Photonic Crystal," Phys. Rev. Lett. **95**, 013904 (2005).
15. S. Strauf, K. Hennessy, M. T. Rakher, Y.-S. Choi, A. Badolato, L. C. Andreani, E. L. Hu, P. M. Petroff, and D. Bouwmeester, "Self tuned quantum dot gain in photonic crystal lasers," Phys. Rev. Lett. **96**, 127404 (2006).
16. T. Yoshie, A. Scherer, J. Hendrickson, G. Khitrova, H. M. Gibbs, G. Rupper, C. Ell, O. B. Shchekin, and D. G. Deppe, "Vacuum Rabi splitting with a single quantum dot in a photonic crystal nanocavity," Nature **432**, 200-203 (2004).
17. M. Nomura, S. Iwamoto, K. Watanabe, N. Kumagai, Y. Nakata, S. Ishida, and Y. Arakawa, "Room temperature continuous wave lasing in photonic crystal nanocavity," Opt. Express **14**, 6308-6315 (2006).
18. B. Ellis, I. Fushman, D. Englund, B. Zhang, Y. Yamamoto, and J. Vučković, "Dynamics of quantum dot photonic crystal lasers," Appl. Phys. Lett. **90**, 151102 (2007).
19. http://www.rsoftdesign.com

1. Introduction

Photonic crystal (PC) slab structures [1, 2] have the ability to control light on a micrometer scale. In general, this control is achieved through two major strategies, each of which exploits a particular property of PCs. The first approach is based on the introduction of a defect in a 2D PC slab. The defect acts as a cavity and creates one or several localized states in the band gap. The careful design of the borders of the cavity can yield very large quality factors and small modal volumes [3]. With this approach, in the presence of a gain medium, lasing can be achieved [4, 5]. The second approach builds upon the enhanced local density of electromagnetic states associated with the critical points of the band dispersion diagram. As the group velocity is small around these points, the electromagnetic interaction between light and matter is greatly enhanced and allows efficient laser operation in the presence of a gain medium. Such lasers have already been demonstrated, generally with quantum wells as a gain medium for in-plane [6, 7] and vertical [8, 9] emission. These two approaches have been combined in different ways, leading to high quality factors and low volume resonant modes which are robust with respect to fabrication imperfections [10, 11, 12]. We propose here to use the approach described in [13], where a photonic bandgap effect is used to confine spatially a valence bandedge mode. We have shown that such a cavity confined slow light mode can exhibit a high quality factor Q and a small mode volume, making it a promising structure for enhancing the radiation dynamics of a source.

By combining high Q factor and low modal volume microcavities with InAs/GaAs quantum dots (QD), different groups have studied various light emission regimes at low temperature, including single photon emission [14], lasing with a small number of quantum dots [15], and observation of strong coupling [16]. In order to achieve laser emission with QDs at room temperature, some authors have proposed to create a stack of QD layers [17]. In this article, we demonstrate *room-temperature* lasing with a *single* InAs/InP QD layer in a suspended membrane. Compared to quantum wells, the use of QDs as gain medium should reduce the threshold as the carrier density at transparency is lower. Incidentally, the β factor, which represents the

#105574 - $15.00 USD Received 8 Jan 2009; revised 20 Feb 2009; accepted 22 Feb 2009; published 20 Mar 2009

proportion of spontaneously emitted photons in the lasing mode, should also be larger with QDs, as the states are discrete, which is another way of decreasing the threshold. However, a detailed study of the experimental β factor is beyond the scope of this work. Another benefit of QDs is that they may exhibit a higher bandwidth when operating in the high-frequency regime [18].

2. Design and fabrication

The photonic structure consists of a 237nm thick InP slab grown by molecular beam epitaxy on top of an InGaAs sacrificial layer. This thickness enables the fabrication of a membrane that behaves like a single mode slab waveguide around 1.5 μm for the TE-like polarization. A single layer of InAs self-organized QDs is grown in the middle of the slab, with a density of 700 μm^{-2}. The InP slab is patterned with circular air holes arranged over a triangular lattice. In the central region, the core, the radius of the air holes is increased such that the frequency of the local valence band edge lies in the photonic band gap of the surrounding crystal (cladding) (Fig. 1). In a previous theoretical study we predicted that this approach would produce fabrication tolerant designs of optical cavities, with Q factors in the 10^5-10^6 range and small mode volumes ($\sim (\lambda/n)^3$) [13].

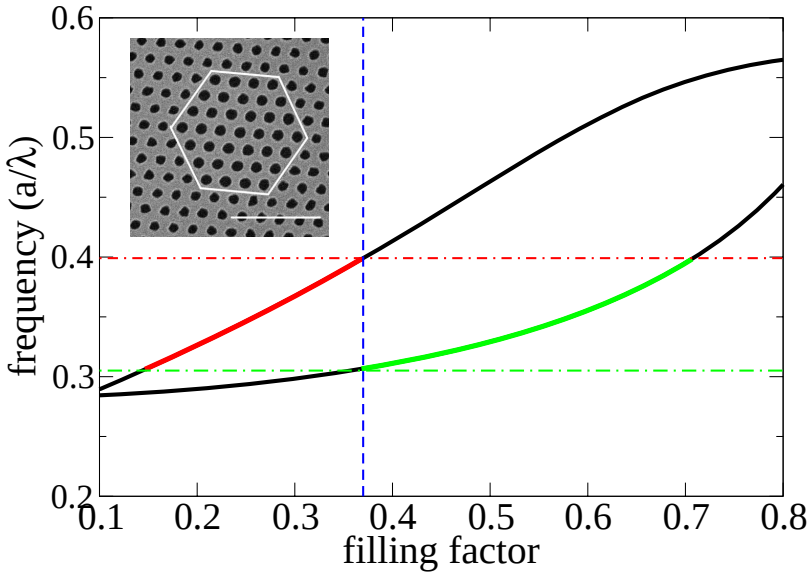

Fig. 1. Evolution of the valence and conduction band edge frequencies with the surface air filling factor for an infinite crystal, computed by 3D plane wave expansion [19]. If, for instance, the cladding region has a filling factor of $f = 0.37$, marked by the vertical blue dashed line, the photonic crystal will possess a bandgap between 0.301 and 0.400. The valence band edge of a crystal with a higher filling factor would then lies in this bandgap (green line). Inset: A typical fabricated structure with a six lattice period wide hexagonal cavity surrounded by a cladding with lower filling factor. The white horizontal line is 2 μm long.

The PC hole pattern is fabricated using e-beam lithography and reactive ion etching, followed by a wet chemical underetching of the sacrificial InGaAs layer to yield a suspended membrane. The period of the lattice is 440nm, with surface air filling factors ranging from 25% to 35% and from 30% to 40% for the cladding and the core, respectively. The cavities are designed such

#105574 - $15.00 USD Received 8 Jan 2009; revised 20 Feb 2009; accepted 22 Feb 2009; published 20 Mar 2009

that the frequency of the cavity mode lies near the maximum of the gain spectrum of the QDs *i.e.* at 1.55 μm.

Optical characterization is carried out using non resonant pulsed optical pumping at 780 nm through a $\times 20$ microscope objective lens at room temperature. The duty cycle of the pump beam is 1% (2ns pulse at a 5MHz repetition rate) to limit temperature increase. The lateral size of the pump beam is 5 μm, which is about twice the size of the cavity. The vertical optical losses pass through the same objective and are collected at the entrance slit of a monochromator.

3. Results and discussion

Most of our fabricated structures support a mode with a full width at half maximum (FWHM) $\delta\lambda$ around 0.2nm. All the structures for which the cavity mode overlaps spectrally with the gain profile of the QDs ($\lambda > 1.5\mu$m) show lasing emission. Depending on the resonant mode wavelength and lifetime, we observed laser thresholds for incident peak power ranging from 300 μW to 6,000 μW.

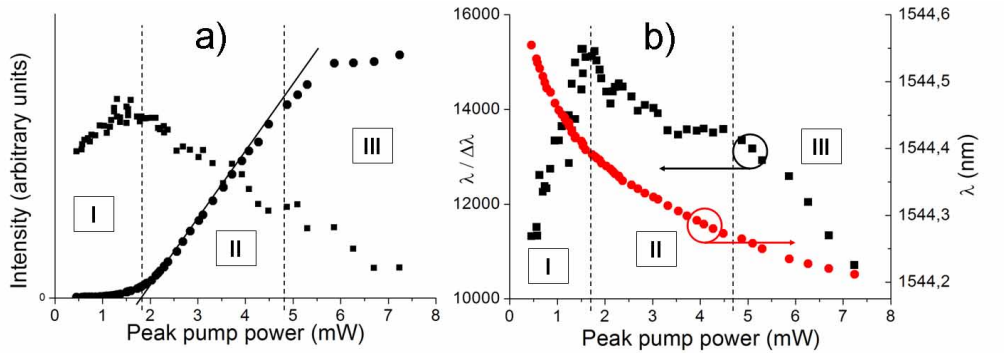

Fig. 2. (a): Lin-Lout curve for the structure S_1 (circles), together with the spontaneous emission background (squares). This quantity is magnified by 100 for clarity; (b): Evolution of the experimental quality factor, defined by $Q_{exp} = \lambda/\delta\lambda$, as described in the text, and of the central wavelength of the mode : λ.

Figure 2 presents the characteristics of one structure, labeled S_1. Its geometrical parameters are $f_{cav} = 37\%$ and $f_{clad} = 31\%$ (core and cladding filling factors respectively). Figure 2(a)) shows the Lin-Lout curve (peak intensity versus peak pump power), together with the spontaneous emission background, defined as the fraction of the energy absorbed by the QDs that is radiated as spontaneous emission, and fig. 2(b)) shows the evolution of the central wavelength of the mode λ, and of the "experimental quality factor", defined as $Q_{exp} = \lambda/\delta\lambda$, where $\delta\lambda$ is the FWHM of the mode peak. Note that Q_{exp} is not the quality factor of the cavity, which should be estimated for a cold cavity, rather it represents a measure of the linewidth of the mode. In the figures, three different regimes can be observed for the evolution of the emitted power as a function of the input power. These regimes correspond to the sections labeled I, II, and III on the Figs. The evolution of the central wavelength λ results from a combination of absorption saturation (blueshift) and temperature increase (redshift). The observed overall monotonic decrease of the central wavelength indicates that the effect of absorption reduction is predominant in the three pumping regimes. Let us consider each regime in detail:

- In the first regime, the amplitude of both the peak of the resonant mode and the background increases with the peak pump power. Photons are spontaneously emitted in the

#105574 - $15.00 USD Received 8 Jan 2009; revised 20 Feb 2009; accepted 22 Feb 2009; published 20 Mar 2009

cavity mode. Q_{exp} also increases as absorption decreases because the increasing peak pump power saturates absorption losses.

- In the second regime, the intensity of the main peak increases linearly. We have a clear evidence of laser emission beyond a threshold of 1.8 mW. Q_{exp} begins to decrease and then stabilizes around 13,500. This behaviour is surprising, as the increase in coherence should make the FWHM decrease. We therefore attribute this behavior to a compromise between two opposite effects: the increase in photons coherence which tends to reduce the linewidth, and the impact of the wavelength shift when the system is driven, i.e. during the pumping phase, which tends to broaden the linewidth of the mode. Since the detection dynamics is much slower, this shift appears as a spectral broadening of the resonance. The wavelength shift is due to a combination between a blue shift, attributed to carrier injection in the InP-based membrane, and a red shift, due to the temperature increase with the pumping power.

- In the third regime, the height of the peak saturates and its linewidth increases. We attribute the clamp of the output to the finite capture rate of the carriers by the QDs, the supernumerary ones being non radiatively recombined in the barriers.

Figure 3 shows the characteristics of a second structure, labeled S_2. Its core consists of five layers of air holes, and its geometrical parameters are $a = 440$nm, $f_{cav} = 39\%$, $f_{clad} = 36\%$ for the period, the core filling factor and the cladding filling factor, respectively.

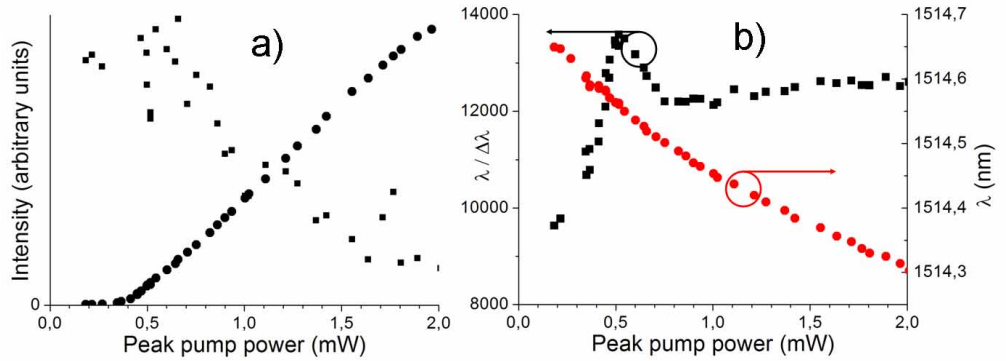

Fig. 3. Characteristics of structure S_2. (a): Lin-Lout curve (disks), together with the spontaneous emission background (squares); (b): Evolution of Q_{exp} and λ.

The single mode lasing operation is achieved with a lasing threshold of 400 μW peak power. Taking into account the reflexion at the surface of the slab, and the filling factor of the core, we estimate that the absorbed power is 20% of the total incident power. This yields an absorbed peak pump power of 80 μW. The duty cycle is 1% (2 ns pulse duration for a 200 ns period), which makes an average total absorbed power of 800 nW. Incidentally, we can observe for S_2 a behaviour similar to structure S_1, except in the third regime. This is because in the case of structure S_2, the input peak pump power did not reach a high enough value to saturate the gain. The value of the experimental quality factor for the saturation regime is about 12,500.

We note that there is a marked difference between the lasing thresholds of the two structures, although their experimental quality factors are similar. In order to investigate this issue we first plot on Fig. 4 the spectra of S_1 (red) and S_2 (blue) together with the photoluminescence of the unpatterned sample. Taking into account a 10 nm Stokes shift, we can deduce from this graph

#105574 - $15.00 USD Received 8 Jan 2009; revised 20 Feb 2009; accepted 22 Feb 2009; published 20 Mar 2009

that the absorption, and consequently the gain, is lower for structure S_1 than for structure S_2, as the two modes lie in the decreasing part of the absorption spectral curve. However this should have only a small influence on the threshold.

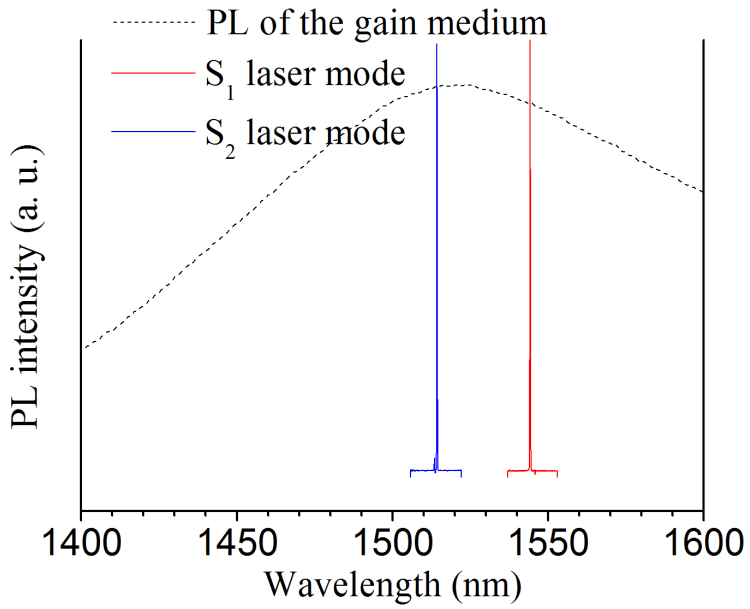

Fig. 4. Photoluminescence of the unstructured sample (in black), corresponding to the QD emission, together with the spectra of the lasing modes of S_1 (red) and S_2 (blue).

Another contribution to the threshold can be understood from 3D finite difference in time domain calculations. Structure S_1 supports a mode at λ=1542 nm, with a Q factor of 220,000, while the mode of structure S_2 is at λ=1514 nm, with a calculated Q factor around 10^6. These calculated Q factors reflect the optical losses only, which are much lower for the mode of S_2 than for the mode of S_1. Although the real Q factors of the photonic structures (with no active material) are probably smaller, as a result of technological imperfections, one may say these theoretical values of the Q factors are in the line of the observed threshold powers.

The calculated Q-factors for the cold cavities are significantly larger than the experimental Q-factors. There are two reasons for this. The first one relates to fabrication imperfections. As can be seen at Fig. 1(a), the holes forming the cladding region are not perfectly circular which entail larger optical losses than what is calculated for a perfect structure. The second limitation of the Q-factors is the presence of absorption, which decreases the observed quality factor. We can write $1/Q = 1/Q_{\text{opt}} + 1/Q_{\text{abs}}$, where Q_{opt} relates to scattering losses and Q_{abs} is a measure of the non-radiative losses due to material absorption. Accordingly, Q can be limited by the absorption above a certain level of losses. In the case of our sample, the absorption is estimated to be $\alpha \approx 10\ cm^{-1}$. By introducing this absorption in the numerical calculations, the obtained Q-factors decrease to the 10^4 range, which matches well the experimental measurements. As the incident pump power is increased, absorption decreases, which leads to an increase in the quality factor, which is observed in the first regime.

#105574 - $15.00 USD Received 8 Jan 2009; revised 20 Feb 2009; accepted 22 Feb 2009; published 20 Mar 2009

4. Conclusion

Using a cavity-confined slow-light mode based on our previous theoretical design we have demonstrated the first suspended photonic crystal InAs/InP quantum dot laser, operating under pulsed excitation, at 1.5 μm at room temperature. The input peak threshold power is 400 μW, which corresponds to an effective absorbed peak power of 80 μW, and to an average threshold power of 800 nW.

Acknowledgment

This work was supported by the Ministère délégué à la Recherche et aux Nouvelles Technologies (Programs "ACI Jeune Chercheur" and "ACN Nanoqub"), and by an award under the Merit Allocation Scheme on the NCI National Facility at the ANU. The authors want to thank Pr. Andrea Fiore for fruitful discussions. Frédéric Bordas is now with COBRA Research Institute, Technische Universiteit Eindhoven.

#105574 - $15.00 USD Received 8 Jan 2009; revised 20 Feb 2009; accepted 22 Feb 2009; published 20 Mar 2009